Tunable normal incidence Ge quantum dot midinfrared detectors

Song Tong,[a] Fei Liu, A. Khitun, and K. L. Wang
Device Research Laboratory, Department of Electrical Engineering, University of California at Los Angeles, Los Angeles, California 90095-1594

J. L. Liu
Quantum Structures Laboratory, Department of Electrical Engineering, University of California at Riverside, Riverside, California 92521

(Received 22 December 2003; accepted 13 April 2004)

Midinfrared photodetectors in the 3–5 μm region were demonstrated by using molecular beam epitaxy grown self-assembled Ge quantum dots at normal incidence. The structure was a *p-i-p* with *p*-type doped Ge dots embedded in the intrinsic layer sandwiched in the two heavily *p*-doped regions. The dark current density at 77 K is 6.4 mA/cm^2 at 1 V. The as-grown sample has a response at normal incidence in the wavelength range of 2.2 to 3.2 μm and peaked at 2.7 μm. Thermal annealing at 900 °C for 10 min shifted the peak response to 3.6 μm. Annealing effect was simulated with the interdiffusion behavior of Ge and Si atoms to explain the shift of the response wavelength.
 [DOI: 10.1063/1.1759081]

I. INTRODUCTION

For midinfrared and far-infrared photodetection, $Hg_xCd_{1-x}Te$ is currently the mainstream material due to its suitable and tunable band gap, which makes it fit for these wavelength ranges. However, this material is well known to have many issues in controlling the growth, the processing, and the fabrication of devices.[1] Thus quantum-well infrared photodetector (QWIP) was proposed and investigated.[2,3] But QWIPs are a one-dimensional confinement system, and are not sensitive to normal incidence light due to the selection rule of intersubband transition. Thus optical coupling through the use of diffraction gratings[4] or random scattering[5] is necessary. In the recent years, quantum dots (QDs) such as InGaAs[6] and Ge[7] dots have been successfully grown by self-assembling processes. QDs are three-dimensional confinement objects and thus can be used for the detection of normal incidence illumination. Quantum dot infrared photodetectors (QDIPs) have attracted a great deal of interest.[8–10] These materials are also predicted to have many advantages such as reduced phonon scattering, longer carrier lifetime, lower dark current, increased optical absorption coefficient, and higher detectivity. Ge quantum dots, comparing to their III–V counterparts, are grown on Si substrates,[6] thus have the potential to be monolithically integrated with the highly advanced Si integrated circuits at low cost. In this paper, we will present our photoresponse results on Ge quantum dots and the controlling of the response wavelength.

II. EXPERIMENT

The sample used for experiment is very much like a *P-I-P* structure, with *p*-type doped Ge dots in the intrinsic Si region, sandwiched by two p^+ regions as contact layers. Double-side-polished highly *p*-type doped Si (100) wafers with a resistivity of 18–25 Ω cm were used as substrates. The substrates were cleaned by using a standard Shiraki method followed by *in situ* thermal cleaning at 930 °C for 15 min. The nominal growth rates are 1 and 0.2 Å/s for Si and Ge, respectively. Boron doping was achieved by sublimation of boron from a Knudsen cell. A 200 nm 5×10^{18} cm^{-3} *p*-doped Si buffer layer was first grown, followed by a 100 nm undoped separation layer with the substrate temperature maintained at 600 °C, then the temperature was reduced to 540 °C during the following growth. Twenty layers of Ge quantum dots were grown separated by 19 undoped Si layers with each layer 20 nm. The nominal thickness of each Ge layer was 1.4 nm and was grown with a boron doping level of 1×10^{18} cm^{-3}. Another 100 nm intrinsic and 200 nm 5×10^{18} cm^{-3} boron doped Si layers were grown on top. The sample was then separated into small pieces for annealing. Annealing was processed with rapid thermal annealing (RTP) in nitrogen at 900 °C for 10 min.

The as-grown and annealed samples were then processed into mesa devices. Mesas were defined by dry etching with CF4/O2 gases and a plasma power of 100 W. The wafers were then treated with BOE:H_2O_2 for 5 min to remove the plasma damaged surface. Low-temperature LPCVD oxide was then deposited for passivation. Contacts using Ti/Al were finally formed by *e*-beam evaporation and lift-off technology. Ohmic contact was formed by 1 min annealing at 400 °C by RTP. The mesa size was 500×500 μm^2. The wafer was diced and the chips were mounted on TO-5 packages for further measurements. *I–V* measurements were carried out with HP4142 in dark. Photoresponse spectra were taken at normal incident geometry. A glow bar operating at 70 W was used as the light source. A 34 cm grating monochromator was used to disperse the light. Photocurrent was measured through a sampling resistor ($R=1.5$ MΩ). A lock-in amplifier was used to detect the voltage signal.

III. RESULTS AND DISCUSSIONS

A cross-sectional transmission electron microscopy (TEM) image of the dot region is shown in Fig. 1. The dot

[a]Author to whom correspondence should be addressed; electronic mail: tong@ee.ucla.edu

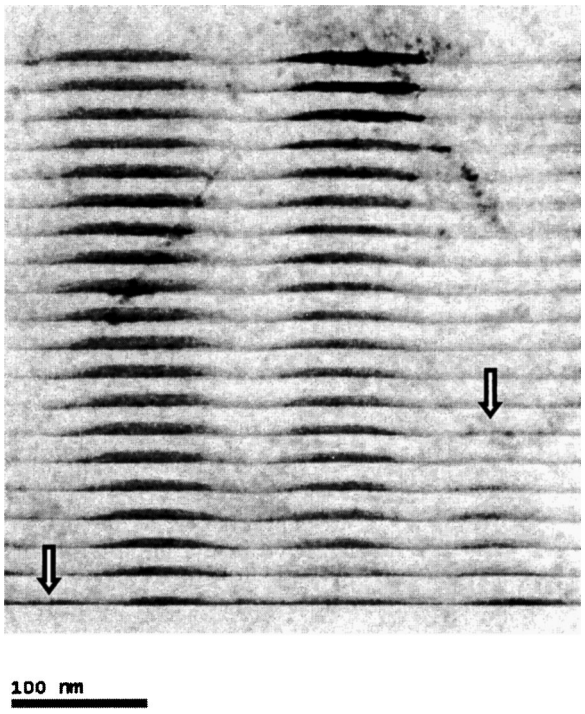

FIG. 1. TEM image of the as-grown sample. Arrows indicate where the dots cease to continue in the upper layers.

height ranges from 7 to 10 nm while the base ranges from 50 to 100 nm. One feature of the structure is that the dots are vertically correlated and form stacks separated by Si separation layers. The vertical correlation shown is typical when the separating Si layer is less than 50 nm. It was established that the underlying dots provide maximum tensile strain for the covering Si and these sites are favorable for forming subsequent dots.[11] As shown in the figure, the dot size increases in upper layers, in both height and base dimensions. The aspect ratio, height:base, is around 1:5–7. It can also be seen that the dot density in the lower layers is large and reduces in the upper layers. Some dot sites appearing in the lower level disappear after one or several layers, as indicated by the arrows in the image.

Figure 2 shows the dark current characteristics of the as-grown QDIP device as a function of the bias voltage at 77 and 300 K. The dark current has an exponential increase with increasing applied bias voltage at moderate biases. This agrees with the theoretical analysis of Ryzhii *et al.*[12] At 77 K, the forward current density at 1 V is 6.4 mA/cm^2. The total dark current consists of three parts, sequential resonant tunneling, thermionic emission, and phonon assisted tunneling.[3] Thermionic hole emission from QDs is the major source for the dark current at these temperatures. The unsymmetrical appearance of the $I-V$ curves is due to the growth induced unsymmetrical properties of the dot region, such as the wetting layer and the dot shape. This is clearly shown in Fig. 1. For the annealed sample, the dark current slightly increases.

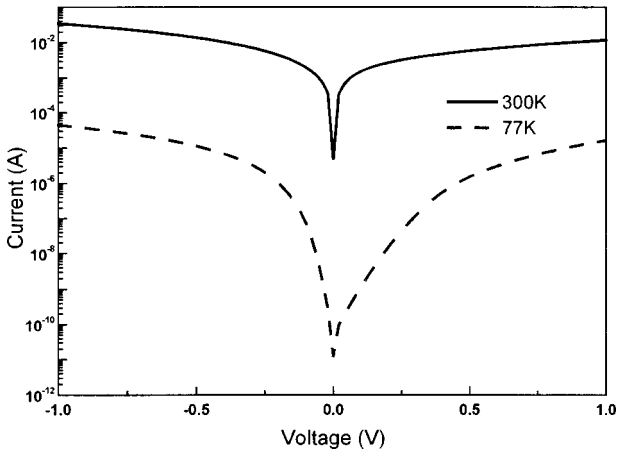

FIG. 2. Current-voltage characteristic of as-grown sample measured at 77 and 300 K.

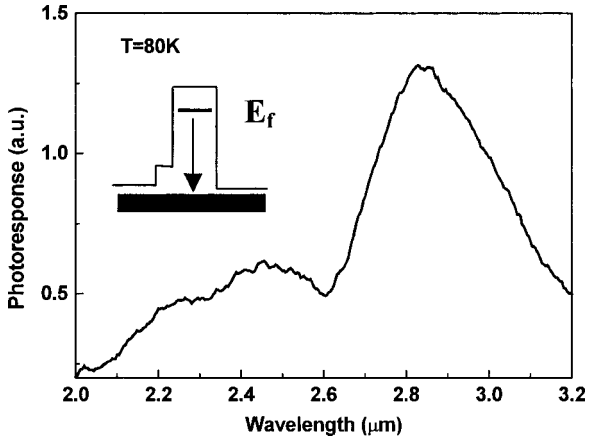

FIG. 3. Photoresponse of the as-grown sample at 80 K. Inset shows the corresponding transition of the holes from the bound states to continuum states.

Figure 3 shows the normal incidence photoresponse spectrum of the as-grown sample measured at 80 K. The response ranges from 2.2 to 3.2 μm and peaked at about 2.7 μm. The full width at half maximum (FWHM) is 0.6 μm, which corresponds to 103 meV, resulting a relatively broad absorption, a linewidth $\Delta\lambda/\lambda$ of 22%. We ascribe this response to the transition of holes in Ge dots from their bound ground states to the continuum states on top of the barrier[13] as illustrated in the inset of Fig. 3. There are many issues that are responsible for the broadening of the spectrum, such as the variation in dot size, Ge content, as well as local strain. From the TEM image, we saw that the dot height and width were different. Our PL results on samples grown at similar conditions show a FWHM of 60 meV,[14] indicating a salient energy variation among the ground states for the dot ensemble. This property is desirable for a wide range response of the detector. On the other hand, the nonuniformity of the dots results in degradation of the absorption intensity since not all the dots participate in the absorption at a certain wavelength.

To move the photoresponse to the more interesting 3–5 μm range, we performed heat treatment to the sample. One sample was annealed at 900 °C for 10 min. The response spectra at different temperatures from 80 to 120 K were shown in Fig. 4. The response spectra range from 2.4 to 4.6 μm and the peak response occurs at 3.6 μm. This shows that

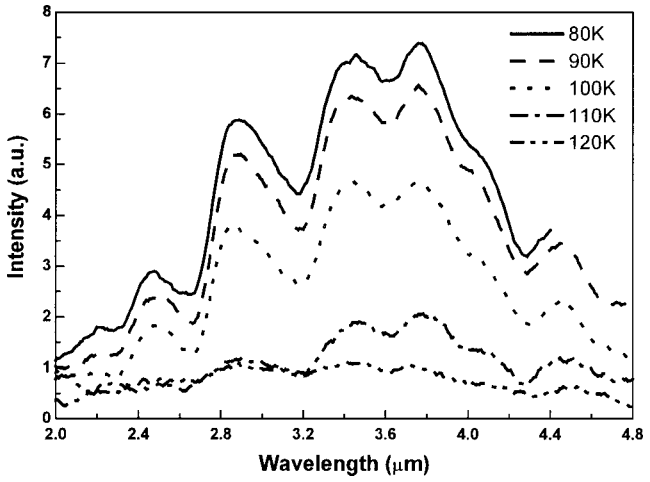

FIG. 4. Photoresponse of the 900 °C and 10 min annealed sample at different temperatures.

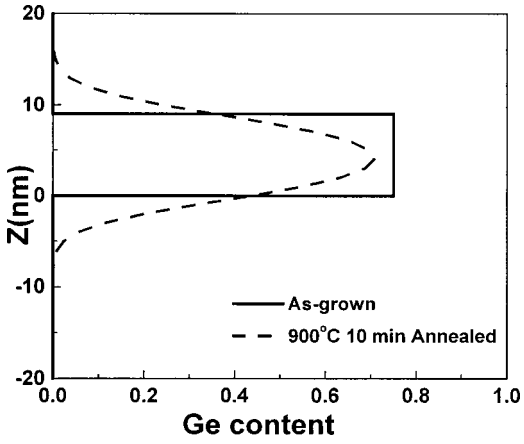

FIG. 5. Simulation results of the Si and Ge interdiffusion at 900 °C for 10 min. $Si_{0.25}Ge_{0.75}$ were assumed for the dot before annealing. The dot was 9 nm in height and 100 nm in base.

annealing may be an effective method to tune the spectral range of quantum dot samples. The result also shows that the response intensity decreases with increasing the temperature. With increasing temperature, the bound holes can be excited out of QD states through thermionic emission. This emission reduces the number of bound carriers that can be photoexcited, thus reduces the photoresponsivity. Another reason may come from the increasing phonon scattering, which can reduce the excited carrier lifetime and reduce the optical gain. The dips in the spectra are due to the interference effect of the epilayer as well as the atmospheric absorption.

The shift of the response wavelength is the result of the interdiffusion of Si and Ge during annealing. In order to estimate the effect of heat treatment on Ge dot composition, we carried out numerical calculations of Ge concentration profile, taking into account Ge/Si interdiffusion processes. The diffusion equation

$$\frac{\partial c}{\partial t} = D\nabla^2 c \tag{1}$$

is solved by the finite differences method and forward time centered step algorithm. In the equation, c is the concentration of Ge atoms, D is the diffusion coefficient, and t is the time. The algorithm is stable only if the so-called Courant-Friedrichs-Lewy condition is met,

$$\tau \leqslant \frac{h^2}{2\max\{D_x, D_y, D_z\}}, \tag{2}$$

where τ and h are time and space steps, respectively. From this condition, it follows that in the nanometer scale ($h \geqslant 1$ nm) and with the diffusion coefficient less than $10^{-15}\,\mathrm{cm}^2/\mathrm{s}$, the computational time step τ must be less than 5 s ($\tau \leqslant 5$ s), which is acceptable as typical annealing time is about several minutes.

In Fig. 5, we show the numerical simulation results of the Ge concentration profile for the SiGe dot embedded in a 100% silicon host matrix. At the initial time the dot is assumed to have 75% Ge. Then, we simulated interdiffusion process for the 10 min annealing. The in-plane diffusion coefficients D_x and D_y are taken to be $10^{-17}\,\mathrm{cm}^2/\mathrm{s}$ ($T \sim 1200$ K) and the diffusion coefficient along the growth axis z is taken to be ten times higher than the in-plane one ($D_z = 10D_x$), as a recent experimental investigation on Ge/Si interdiffusion in GeSi dots has shown a significant diffusion anisotropy.[15] One can see a significant "broadening" of the initial quantum dot region as a result of interdiffusion from the initial steplike Ge distribution to a Gaussian-like shape. After annealing, the average Ge content in the original dot site decreases to 58% from the initial 75%. This can be confirmed by our former TEM results.[16] Evidently, interdiffusion substantially modifies the dot physical and electrical structure. In this simulation, we neglected the following effects. First, we assumed that initially the dot has a uniform Ge distribution, yet, in fact, the Ge content in the GeSi dots is not uniform and usually the dots tend to have Ge-rich cores.[17] Second, we did not include the effects of strain and Ge concentration on the diffusion coefficients, as there are no sufficient experimental data on these parameters. Nevertheless, this simulation still provides useful information to predict the effect of thermal treatment on dot electronic and optical properties.

As we have pointed out previously, the optical transitions are from the bound heavy hole states to continuum states. To evaluate this energy level, a three-dimensional valence band finite deep potential box model with effective mass approximation was used. We calculated the response wavelength dependence on dot parameters, i.e., Ge content, strain, QD height, and base width. Since quantum dots are partially relaxed,[18] a strain ratio $(a_{\|\mathrm{dot}} - a_{\mathrm{Si}})/(a_{\mathrm{SiGe}} - a_{\mathrm{Si}})$ is used to describe the percentage of strain in QDs. First, the effective masses of relaxed SiGe alloys were obtained by using the Vegard's law $1/m^*_{\mathrm{SiGe}} = x/m^*_{\mathrm{Ge}} + (1-x)/m^*_{\mathrm{Si}}$. Then, the change of effective mass due to strain was obtained by using a two band k^*p method. The valence band offset of $Si_{1-x}Ge_x$ strained layers on (100) Si substrate were taken from the results of Rieger and Vogl.[19] In Fig. 6 we show the response wavelength dependence on Ge content and strain. The dot height and base were taken to be 9 and 100 nm, respectively. The four curves correspond to four values of relative strain in the dot, 100%, 80%, 60%, and 40%. The

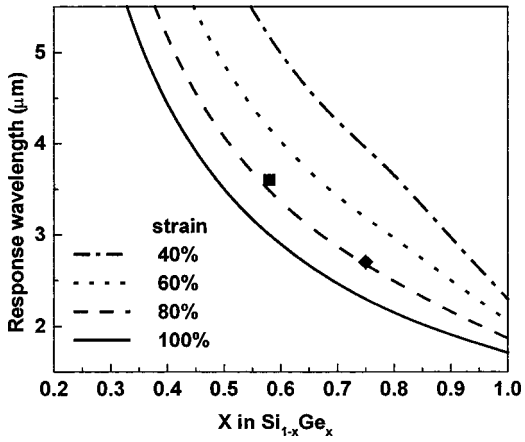

FIG. 6. Calculated results on the peak response wavelength dependent on the Ge content and Ge QDs strain ratio for QDs with the height of 9 nm and the base of 100 nm. The diamond and square signs indicate the points for the as-grown sample and the annealed sample, respectively.

calculation results show that lower Ge content in QD and smaller QD strain ratio are necessary in order to achieve longer wavelength response. At the growth temperature of 540 °C, we can estimate the Ge content in the dot to be 75%.[20,21] Considering this together with the response peak of 2.7 μm, we can proceed to determine the relative strain to be about 65%. This point is denoted by the diamond sign in the plot. The point after annealing is also shown in the plot as a square sign. We can see that the relative strain keeps about the same value as before annealing. This means that the absolute strain value decreased since the Ge content decreased. The calculation also shows that the peak wavelength changes about 17% as the dot height increases from 3 nm to 9 nm for a constant Ge content and strain. The response wavelength has a weak dependence on the base dimension since the base dimension is much larger than the height.

As we have seen, one effect of annealing is the interdiffusion between Ge and Si, the Ge content in the quantum dot decreases after annealing. The second effect is to make the QDs become more relaxed. Both effects lead to a smaller valance band offset and thus the response shifts to longer wavelength. Another effect is that QD becomes larger and this will give shorter wavelength response. However, our calculations show that the variation of QD height at around 9 nm has a relatively weak effect on the response wavelength for QD comparing to those due to Ge content and QD strain.

Besides the postannealing process that we investigated here, by varying the Ge deposition thickness, the energy levels can also be tuned. We observed a 28 meV peak energy shift in photoluminescence spectra for samples grown with 1.2 and 1.5 nm Ge. Comparing to the 115 meV shift for the rapid annealing, this method is relatively less effective.

The absorption coefficient of this kind of devices was studied using identical structure grown on lowly doped Si double side polished substrate with waveguide geometry. The results show an absorption coefficient of 5800 cm^{-1}. This value is high comparing to the III–V quantum wells, which is typically 400–1800 cm^{-1},[3] presumably due to the high doping density in our structure. Research is going on to investigate the absolute responsivity in our laboratory.

VI. CONCLUSION

Molecular beam epitaxy grown Ge dots photodetectors were fabricated. The *p-i-p* structure showed normal incident photoresponse. As-grown samples had a response range from 2.2 μm to 3.2 μm. Annealing was shown to be able to tune the response to longer wavelength range, i.e., 2.5–4.8 μm for 900 °C 10 min annealed samples. The normal incident response from boron-doped Ge QDs was ascribed to transitions from heavy hole ground states to continuum states in the valence band. The dark current density at 1 V was 6.4 mA/cm^2 at 77 K, which could be optimized by tuning the doping level and the spacing layer thickness in the active region. The response wavelength calculations agree with the experimental results. It was also pointed out that lower Ge content and smaller dots are more favorable for the longer wavelength range response. To achieve this, smaller nominal Ge growth thickness and relatively higher growth temperatures can be used. In addition, by using laser annealing, the same tuning results may be obtained at selected areas, and this can give a matrix of photodetectors with different response peaks. Ge quantum dot arrays on Si substrate may find potential application for midinfrared photodetectors.

ACKNOWLEDGMENTS

Financial support by MURI under the Centroid project and phonon program is gratefully acknowledged.

[1] A. Sher, M. A. Berding, M. van Schilfgaarde, and C. An-Ban, Semicond. Sci. Technol. **6**, C59 (1991).
[2] L. Esaki and H. Sakaki, IBM Tech. Discl. Bull. **20**, 2456 (1977).
[3] B. F. Levine, J. Appl. Phys. **74**, R1 (1993).
[4] D. Heitmann and U. Mackens, Phys. Rev. B **33**, 8269 (1986).
[5] E. Yablonovitch and G. D. Cody, IEEE Trans. Electron Devices **ED-29**, 300 (1982).
[6] D. Leonard, M. Krishnamurthy, C. M. Reaves, S. P. Denbaars, and P. M. Petroff, Appl. Phys. Lett. **63**, 3203 (1993).
[7] H. Sunamura, S. Fukatsu, N. Usami, and Y. Shiraki, J. Cryst. Growth **157**, 265 (1995).
[8] V. Ryzhii, Semicond. Sci. Technol. **11**, 759 (1996).
[9] P. Bhattacharya, A. D. Stiff-Roberts, S. Krishna, and S. W. Kennerly, SPIE-Int. Soc. Opt. Eng. Proceedings of SPIE, International Society for Optical Engineering, **46**, 100 (2002).
[10] H. C. Liu, M. Gao, J. McCaffrey, Z. R. Wasilewski, and S. Fafard, Appl. Phys. Lett. **78**, 79 (2001).
[11] O. G. Schmidt, O. Kienzle, Y. Hao, K. Eberl, and F. Ernst, Appl. Phys. Lett. **74**, 1272 (1999).
[12] V. Ryzhii, V. Pipa, I. Khmyrova, V. Mitin, and M. Willander, Jpn. J. Appl. Phys., Part 2 **39**, L1283 (2000).
[13] B. F. Levine, A. Zussman, S. D. Gunapala, M. T. Asom, J. M. Kuo, and W. S. Hobson, J. Appl. Phys. **72**, 4429 (1992).
[14] S. Tong, J. L. Liu, J. Wan, and K. L. Wang, Appl. Phys. Lett. **80**, 1189 (2002).
[15] J. Wan, Y. H. Luo, Z. M. Jiang, G. Jin, J. L. Liu, K. L. Wang, X. Z. Liao, and J. Zou, J. Appl. Phys. **90**, 4290 (2001).
[16] J. Wan, Y. H. Luo, Z. M. Jiang, G. Jin, J. L. Liu, K. L. Wang, X. Z. Liao, and J. Zou, Appl. Phys. Lett. **79**, 1980 (2001).
[17] J. Tersoff, Phys. Rev. Lett. **81**, 3183 (1998).
[18] Z. M. Jiang, X. M. Jiang, W. R. Jiang, Q. J. Jia, W. L. Zheng, and D. C. Qian, Appl. Phys. Lett. **76**, 3397 (2000).
[19] M. M. Rieger and P. Vogl, Phys. Rev. B **48**, 14276 (1993).
[20] J. L. Liu, J. Wan, Z. M. Jiang, A. Khitun, K. L. Wang, and D. P. Yu, J. Appl. Phys. **92**, 6804 (2002).
[21] G. Capellini, M. De Seta, and F. Evangelisti, Appl. Phys. Lett. **78**, 303 (2001).